

See discussions, stats, and author profiles for this publication at: <https://www.researchgate.net/publication/275830161>

Branched Amino Acid Based Poly(ester urea)s with Tunable Thermal and Water Uptake Properties

ARTICLE *in* MACROMOLECULES · APRIL 2015

Impact Factor: 5.8 · DOI: 10.1021/acs.macromol.5b00376

READS

46

3 AUTHORS, INCLUDING:



Jiayi Yu

University of Akron

8 PUBLICATIONS 54 CITATIONS

[SEE PROFILE](#)

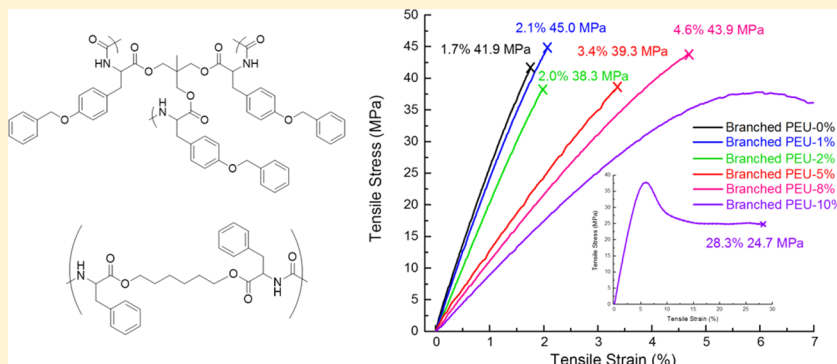
Branched Amino Acid Based Poly(ester urea)s with Tunable Thermal and Water Uptake Properties

Jiayi Yu,[†] Fei Lin,[†] and Matthew L. Becker^{*,†,||}

[†]Department of Polymer Science, The University of Akron, Akron, Ohio 44325, United States

^{||}Department of Biomedical Engineering, The University of Akron, Akron, Ohio 44325, United States

 Supporting Information



ABSTRACT: A series of amino-acid based poly(ester urea)s (PEU) with controlled amounts of branching was synthesized and characterized. The mechanical properties, thermal characteristics and water absorptions varied widely with the extent of branch unit incorporation. Herein, the details of the synthesis of a linear bis(L-phenylalanine)-hexane 1,6-diester monomer, a branch tri-O-benzyl-L-tyrosine-1,1,1-trimethylethane triester monomer and a series of copolymers are described. The extent of branching was varied by adjusting the molar ratio of linear to branched monomer during the interfacial polymerization. The elastic moduli span a range of values (1.0–3.1 GPa) that overlaps with several clinically available degradable polymers. Increasing the amount of branching monomers reduces the molecular entanglement, which results in a decrease in elastic modulus values and an increase in values of elongation at break. The L-phenylalanine-based poly(ester urea)s also exhibited a branch density dependent water uptake ability that varied between 2 and 3% after 24 h of immersion in water. Nanofibers incorporating 8% branching were able to maintain their morphology at elevated temperature, in hydrated conditions, and during ethylene oxide sterilization which are critical to efforts to translate these materials to clinical soft tissue applications.

INTRODUCTION

Macromolecular architecture has been recognized as an important tool to obtain polymers with tailored properties.^{1–3} Materials exhibiting a distinct relationship between molecular architecture and macroscopic properties include dendrimers and hyperbranched polymers. Collectively these works clearly demonstrate that introducing branching units into linear polymers can dramatically change the physical properties. Dendrimers and hyperbranched polymers possess unique three-dimensional chemical structure and have potential applications in coatings,^{4–7} additives,^{4,8} catalysts,^{2,9} drug delivery systems,^{10–14} and bioimaging systems.^{2,9,15,16} Unlike linear polymers, dendrimers and hyperbranched polymers exhibit unique properties including non/low chain entanglements,^{17,18} low viscosity,^{9,18,19} high solubility,^{2,14,18,20} unusual self-assembly behavior,^{2,10,21,22} large number of terminal groups that can be chemically modified and large capacity of encapsulation for guest molecules.^{1,2,10,23,24} Despite the well-defined monodisperse architecture of dendrimers, scalability challenges have limited widespread clinical and commercial applications.²⁴ In

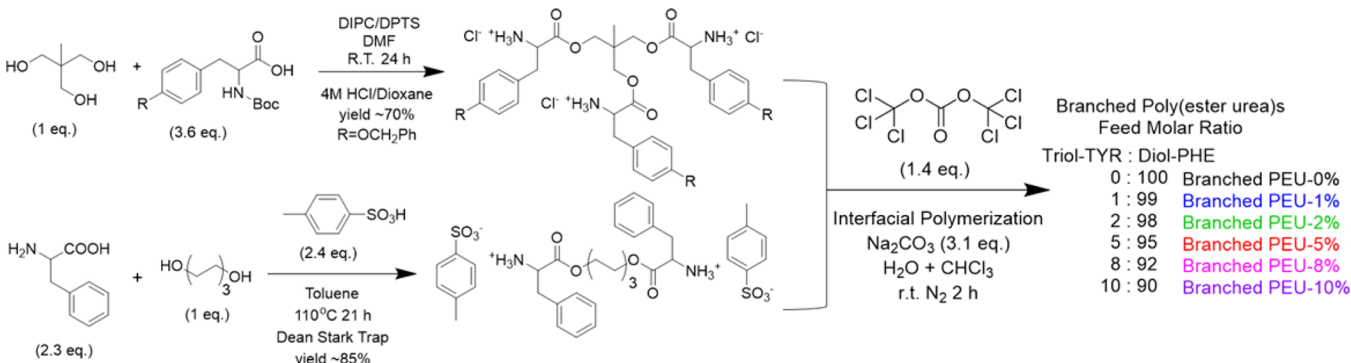
contrast, hyperbranched polymers can be conveniently synthesized on large scales in one-pot reactions using step growth,^{17,18,25–32} ring-opening polymerization,^{17,18,25} requiring little or no additional purification.^{24,33} Thus, hyperbranched polymers not only retain some of the structural features and properties of dendrimers but they are more accessible commercially.

Hyperbranched polymers, especially degradable versions, such as polyethers, polyesters, polyphosphates and polysaccharides have found increasing use in material science and bioengineering applications. Hyperbranched polymers, especially those synthetic biodegradable hyperbranched polymers, have been receiving more and more attention in materials science as well as in biomedical science, including hyperbranched polyethers, polyesters, polyphosphates, polysaccharides. Hult and Penczek first reported the synthesis of

Received: February 20, 2015

Revised: April 7, 2015

Scheme 1. Two-Step General Synthetic Route of Branched Poly(ester urea)s Using Interfacial Polymerization (Branched PEU-0%, Branched PEU-1%, Branched PEU-2%, Branched PEU-5%, Branched PEU-8%, and Branched PEU-10%)^a



^aThe hexanediol (1 equiv) is reacted with L-phenylalanine (2.3 equiv) that has already been protonated by p-toluenesulfonic acid to prevent amidation and exchange reactions during the linear monomer synthesis. The branched monomer is synthesized by the esterification between Boc-O-benzyl-L-tyrosine (1 equiv) and 1,1,1-tri(hydroxymethyl)ethane (3.6 equiv). Following the diamine/triamine synthesis, interfacial polycondensation with triphosgene yields the branched poly(ester urea)s with different branch densities.

hyperbranched aliphatic polyethers, poly(3-ethyl-3-oxetanemethanol), by a cationic ring-opening polymerization.^{34,35} Frey and his colleagues used anionic ring-opening multibranching polymerization to obtain a hyperbranched polyglycerol.³⁶ Kricheldorf et al. reported the potentially biodegradable homo- and copolyesters from gallic acid, phloretic acid and vanillic acid.^{37–39} Van Benthem et al. and Li et al. reported the synthesis of hyperbranched poly(ester amide)s via direct polycondensation from commercially available aliphatic carboxylic anhydrides and multihydroxyl primary amines.^{40,41} Liu et al. synthesized hyperbranched polyphosphates using self-condensing ring-opening polymerization of cyclic phosphate monomers 2-(2-hydroxyethoxy)ethoxy-2-oxo-1,3,2-dioxaphospholane without catalyst.⁴² All of these hyperbranched polymers have shown potentials in the self-assembly of micelles and biomedical applications.^{42–44}

α -Amino acid based poly(ester urea)s have proven to be important materials for biomedical applications because of their excellent blood, tissue compatibility and nontoxic hydrolysis byproducts.^{45–48} Their semicrystalline structure provides a nonchemical method to enhance their mechanical properties and processing characteristics. Also, their synthetic flexibility yields a diverse physical and chemical landscape that is available for exploration.⁴⁹ We have previously demonstrated the synthesis of a 1,6-hexanediol L-phenylalanine-based PEU, poly(1-PHE-6), that possesses an elastic modulus (6.1 GPa) nearly double that of poly(lactic acid) (2.9 GPa)⁵⁰ and when cross-linked with osteogenic growth peptide maintain potent osteoinductive activity.⁵¹ Significantly, there was no evidence of inflammation due to acidification arising during the degradation of poly(1-PHE-6) implanted *in vivo*.^{51–53} We have also developed a series of linear L-phenylalanine-based PEU that possess variations in diol chain length that result in tunable mechanical properties, thermal characteristics and degradation rates.⁵⁴ The mechanical data span a range of values that overlaps with several currently clinically available degradable polymers and the materials exhibited a diol length dependent degradation process that is tunable. In addition, the synthesis of PEU nanofibers carrying pendent “clickable” groups including alkyne, azide, alkene, tyrosine–phenol, and ketone groups on modified tyrosine amino acids were reported. A series of bioactive peptides and fluorescent molecules were conjugated

to the surface of nanofibers following electrospinning using bio-orthogonal reactions in aqueous media.^{55,56}

In this paper, the synthesis and characterization of a linear monomer, a branched monomer and a series of strong and biodegradable branched poly(ester urea)s are described. We have systematically varied the amount of branched monomer incorporated into the copolymers and measured the mechanical properties and water uptake abilities of the resulting branched poly(ester urea)s. A two-step synthetic interfacial polycondensation was utilized to obtain high molecular-weight polymers with high yield. The chemical structures were confirmed by ¹H NMR, ¹³C NMR, ESI and FTIR. The thermal properties were tested by TGA and DSC. The mechanical properties were studied using tensile tests (Instron) at room temperature. The extent of water uptake was measured using a solvent exchange approach with a Quartz Crystal Microbalance (QCM) and compared with the control group of poly(ϵ -caprolactone) (PCL). Nanofibers of branched PEU-8% were prepared via electrospinning. The morphology of the nanofibers incubated in different conditions was confirmed by the field-emission scanning electron microscopy (SEM) images. All the above characterization data suggest that these materials will enable further development of scaffolds for regenerative medicine with improved mechanical properties.

EXPERIMENTAL SECTION

Materials. All chemicals and reagents were purchased from Sigma or Fisher Scientific and used as received unless noted otherwise. Chloroform was distilled after drying overnight with calcium hydride.

General Procedures. The 300 or 500 MHz ¹H NMR and 75 or 125 MHz ¹³C NMR spectra were recorded using a Varian NMR spectrophotometer. All chemical shifts were reported in ppm (δ), and referenced to the chemical shifts of the residual solvent resonances (¹H NMR DMSO- d_6 2.50 ppm; ¹³C NMR DMSO- d_6 39.50 ppm). The following abbreviations were used to explain the multiplicities: s = singlet, d = doublet, t = triplet, br = broad singlet, and m = multiplet. FTIR of all compounds were recorded using MIRACLE 10, Shimadzu Corp. ATR-FTIR spectrometer with 4 cm⁻¹ resolution. Electrospray ionization (ESI) was performed using a HCT Ultra II quadrupole ion trap mass spectrometer (Bruker Daltonics, Billerica, MA) equipped with an electrospray ionization source. Number-average molecular mass (M_n), weight-average molecular mass (M_w), and postprecipitation molecular mass distribution (D_M) were determined by size exclusion chromatography (SEC). The SEC analyses were performed

using a TOSOH HLC-8320 gel permeation chromatograph instrument. The experiments were carried out with a flow rate of 1 mL/min using HPLC grade *N,N*-dimethylformamide (DMF) with 25 mM LiBr as the eluent at 323 K with a refractive index (RI) detector and molecular mass values were determined relative to polystyrene standards. The SEC analyses were also performed using a Varian 390-LC-Multi detector suite system equipped with a PLGel 3 μ m (50 \times 7.5 mm) guard column, two PLGel 5 μ m (300 \times 7.5 mm) mixed-C columns, and a PLAST RT autosampler. Detection was conducted using a dual angle light scattering detector (15° and 90°). The analyses were performed in HPLC grade DMF with 5 mM NH₄BF₄ as the eluent at 323 K and at a flow rate of 1.0 mL/min. A single narrow molecular weight poly(methyl methacrylate) standard (73.15 kDa, dn/dc = 0.069, IV = 0.267) was used to calibrate for absolute molecular weight. The thermal stability of the polymers was measured using thermogravimetric analysis (TGA, TA Q500) across a temperature range of 0 to 600 °C at a scanning rate of 20 °C under nitrogen. The thermal characteristics of the polymers were determined using differential scanning calorimetry (DSC, TA Q2000) from 0 to 220 °C at a scanning rate of 20 °C/min. The resulting values of the thermal properties were determined from three individual measurements. The glass transition temperature was determined from the midpoint in the second heating cycle of DSC.

Synthesis of Di-*p*-toluenesulfonic Acid Salts of Bis(L-phenylalanine)-Hexane 1,6-Diester Monomer. (Diol-PHE). Di-*p*-toluenesulfonic acid salts of bis(L-phenylalanine)-diol diester monomers were prepared using procedures published previously,^{54–57} as shown in Scheme 1. (¹H NMR in Figure 1, ¹³C NMR, ESI mass spectra and FTIR in Figures S1, S2, and S4, Supporting Information)

In brief, 1,6-hexanediol (10.0 g, 90 mmol, 1.0 equiv), L-phenylalanine (32.2 g, 200 mmol, 2.3 equiv), *p*-toluenesulfonic acid monohydrate (38.7 g, 200 mmol, 2.4 equiv), and toluene (200 mL) were mixed in a 500 mL 2-neck round-bottom flask equipped with Dean–Stark trap and a magnetic stir bar. The system was heated to reflux (110 °C) and purged with nitrogen for 20 h. After 20 h, the reaction mixture was cooled to ambient temperature and the product was filtered with diethyl ether. The solid product was dissolved in 3 L of hot water and decolorized using activated carbon black (2.0 g) for 2–3 min. Then, a decolorized hot liquid was obtained by vacuum filtration. When cooled to room temperature, a white solid product would be obtained by vacuum filtration. The solid product was recrystallized 3 times using 3L of water to yield 57.0 g (yield 85%) of di-*p*-toluenesulfonic acid salt of bis-L-phenylalanine-1, 6-hexanediol-diester as a white powder. ¹H NMR (300 MHz, DMSO-*d*₆): 1.04–1.13 (m, 4H, –COOCH₂CH₂CH₂–) 1.38–1.44 (m, 4H, –COOCH₂CH₂CH₂–) 2.27 (s, 6H, CH₃Ar–) 2.50 (DMSO) 2.98–3.19 (m, 4H, –CHCH₂–Ar–) 3.89–4.03 (m, 4H, –COOCH₂CH₂–) 4.25–4.32 (m, 2H, ¹NH₃CHCOO–) 7.09–7.13 (d, 4 H, aromatic H) 7.21–7.34 (m, 10H, aromatic H) 7.47–7.50 (d, 4H, aromatic H) 8.36 (s, 6H, ¹NH₃–). ¹³C NMR (75 MHz, DMSO-*d*₆): 20.75, 24.66, 27.62, 35.97, 38.80–40.28 (DMSO-*d*₆), 53.07, 65.46, 125.39, 127.14, 127.95, 128.49, 129.30, 134.69, 137.78, 145.33, 169.03.

Synthesis of Hydrochloric Acid Salts of Tri-O-benzyl-L-tyrosine-1,1,1-trimethylethane Triester Monomer. (Triol-TYR). The branched monomer was synthesized through the esterification between Boc-O-benzyl-L-tyrosine and 1,1,1-tri(hydroxymethyl)ethane, as shown in Scheme 1. (¹H NMR in Figure 1, ¹³C NMR, ESI mass spectra, and FTIR in Figures S1, S3, and S4)

1,1,1-Tri(hydroxymethyl)ethane (1.00 g, 8 mmol, 1.0 equiv), Boc-O-benzyl-L-tyrosine (11.10g, 30 mmol, 1.2 \times 3 equiv) and 4-(*N,N*-dimethylamino)puridinium 4-toluenesulfonate (DPTS, 1.50 g, 5 mmol, 0.6 equiv) were dissolved in a minimum amount of DMF. After reaction immersion in an ice bath for 10 min, 1,3-diisopropyl carbodiimide (DPIC, 5.7 mL, 40 mmol, 1.5 \times 3 equiv) was added via syringe. A light yellow precipitate was observed in minutes. The reaction was allowed to warm up to room temperature and kept stirring for 24 h. After removing DMF under reduced pressure, the solid was dissolved in chloroform and washed with sodium bicarbonate solution three times. The collected organic solution was concentrated for chromatography purification on silica gel (ethyl acetate/hexane =

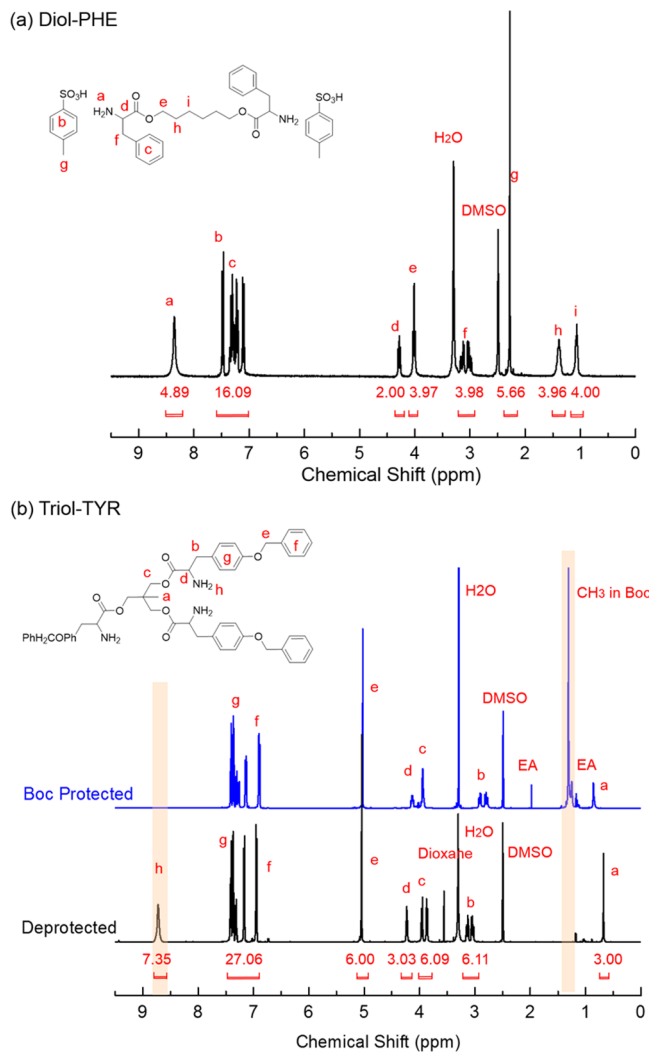


Figure 1. ¹H NMR (DMSO-*d*₆) of di-*p*-toluenesulfonic acid salts of bis(L-phenylalanine)-hexane 1,6-diester monomer (Diol-PHE) and hydrochloric acid salts of tri-O-benzyl-L-tyrosine-1,1,1-trimethylethane triester monomer (Triol-TYR).

1:2 v/v). The resulting product was a light yellow solid (8.4 g, yield 72%). ¹H NMR (500 MHz, DMSO-*d*₆): 0.86 (s, 3H, –CCH₃), 1.31 (s, 27H, CH₃ in Boc protecting group), 2.50 (DMSO), 2.77–2.93 (d, 6H, –CHCH₂–Ar–), 3.92–3.97 (m, 6H, –COOCH₂C–), 4.11–4.16 (m, 3H, ¹NH₃CHCOO–), 5.03 (s, 6H, –Ar–OCH₂–Ar), 6.89–7.42 (m, 27H, aromatic H).

Boc-protected precursors were dissolved in HCl/dioxane (4 M) and kept stirring under nitrogen for 12 h. A 8.5 g sample of light yellow solid (yield 70%) was obtained by freeze-dry to remove the solvent. ¹H NMR (300 MHz, DMSO-*d*₆): 0.68 (s, 3H, –CCH₃), 2.50 (DMSO), 3.02–3.06 (m, 3H, –CHCH₂–Ar–), 3.12–3.16 (m, 3H, –CHCH₂–Ar–), 3.85–3.97 (d, 6H, –COOCH₂C–), 4.22–4.24 (m, 3H, ¹NH₃CHCOO–), 5.03 (s, 6H, –Ar–OCH₂–Ar), 6.93–7.43 (m, 27H, aromatic H), 8.72 (s, 9H, ¹NH₃–). ¹³C NMR (75 MHz, DMSO-*d*₆): 16.45, 35.43, 38.18, 39.68–40.52 (DMSO-*d*₆), 53.90, 66.64–66.81, 69.66, 115.37, 127.34, 128.85–128.89, 130.86, 137.55, 158.03, 168.86.

Synthesis of Branched Poly(ester urea)s. The branched poly(ester urea)s were synthesized by interfacial polymerization. In brief, the di-*p*-toluenesulfonic acid salt of bis(L-phenylalanine)-hexane 1,6-diester monomer (Diol-PHE) and hydrochloric acid salts of tri-O-benzyl-L-tyrosine-1,1,1-trimethylethane triester monomer (Triol-TYR) with molar ratio of 100:0, 99:1, 98:2, 95:5, 92:8, 90:10, respectively (1.0 equiv. in total), and sodium carbonate anhydrate (2.1 equiv) were

dissolved in distilled water (0.1 M for monomer) in a 2 L 3-neck round-bottom flask. The mixture was stirred in a 35 °C water bath for 0.5 h using mechanical stirring. An ice bath was used to cool the system to 0 °C. Several minutes later, additional sodium carbonate (1.05 equiv) was dissolved in distilled water and the solution was transferred into the 2 L 3-neck round-bottom flask. When the solution in the flask turned to a clear state, triphosgene (0.35 to 1.0 equiv of monomer in total) was dissolved in freshly distilled chloroform (0.6 M) and the mixture was added into the 2 L 3-neck round-bottom flask through an addition funnel as quickly as possible. The solution in the flask turned white immediately. After 0.5 h, an additional aliquot of triphosgene (0.08 equiv) was dissolved in freshly distilled chloroform (0.6 M) and transferred into the flask dropwise through an addition funnel. The drop rate was approximately 1 drop per second. After 2 h, the solution in the flask was transferred to a separatory funnel. After washing with water, the organic phase was precipitated into hot water. After cooling and drying, polymer (yield 90%) was obtained.

Branched PEU-0% (*Bis(L-phenylalanine)-Hexane 1,6-Dieste Monomer and Tri-O-benzyl-L-tyrosine-1,1,1-trimethylethane Triester Monomer with a Molar Ratio of 100:0*). ^1H NMR (500 MHz, DMSO- d_6): 1.15 (m, 4H, $-\text{COOCH}_2\text{CH}_2\text{CH}_2-$), 1.43 (m, 4H, $-\text{COOCH}_2\text{CH}_2\text{CH}_2-$), 2.5 (DMSO), 2.87–2.94 (m, 4H, $-\text{CHCH}_2\text{Ar}-$), 3.94 (m, 4H, $-\text{CHCOOCH}_2\text{CH}_2-$), 4.34–4.40 (m, 2H, $-\text{NHCHCOO}-$), 6.47–6.5 (m, 2 H, $-\text{NH}-$), 7.14–7.17 (m, 4H, aromatic), 7.19–7.28 (d, 6H, aromatic). ^{13}C NMR (75 MHz, DMSO- d_6): 25.33, 28.38, 38.10, 39.40–40.56 (DMSO), 54.49, 64.65, 127.04, 128.78, 129.65, 137.34, 157.07, 172.89.

Branched PEU-1%, branched PEU-2%, branched PEU-5%, branched PEU-8%, and branched PEU-10% possess NMR shifts corresponding to the bis(*L*-phenylalanine)-hexane 1,6-diester monomer units are identical as branched PEU-0%. The chemical shifts of tri-*O*-benzyl-*L*-tyrosine-1,1,1-trimethylethane triester monomer units are described below.

Branched PEU-1% (*Bis(L-phenylalanine)-Hexane 1,6-Dieste Monomer and Tri-O-benzyl-L-tyrosine-1,1,1-trimethylethane Triester Monomer with a Molar Ratio of 99:1*). ^1H NMR (500 MHz, DMSO- d_6): 0.72–0.76 (m, 3H, $-\text{CCH}_3$), 4.29 (m, 3H, $-\text{NHCHCOO}-$), 4.99–5.02 (m, 6H, $-\text{ArOCH}_2\text{Ar}-$), 6.33–6.35 (m, 3H, $-\text{NH}-$), 6.86–7.08 (m, BzI unit aromatic H), 7.33–7.41 (shoulder, tyrosine unit aromatic H).

Branched PEU-2% (*Bis(L-phenylalanine)-Hexane 1,6-Dieste Monomer and Tri-O-benzyl-L-tyrosine-1,1,1-trimethylethane Triester Monomer with a Molar Ratio of 98:2*). ^1H NMR (500 MHz, DMSO- d_6): 0.72–0.76 (m, 3H, $-\text{CCH}_3$), 4.26–4.29 (m, 3H, $-\text{NHCHCOO}-$), 4.99–5.02 (m, 6H, $-\text{ArOCH}_2\text{Ar}-$), 6.33–6.35 (m, 3H, $-\text{NH}-$), 6.86–7.08 (m, BzI unit aromatic H), 7.32–7.42 (shoulder, tyrosine unit aromatic H).

Branched PEU-5% (*Bis(L-phenylalanine)-Hexane 1,6-Dieste Monomer and Tri-O-benzyl-L-tyrosine-1,1,1-trimethylethane Triester Monomer with a Molar Ratio of 95:5*). ^1H NMR (500 MHz, DMSO- d_6): 0.72–0.76 (m, 3H, $-\text{CCH}_3$), 4.29 (m, 3H, $-\text{NHCHCOO}-$), 4.99–5.02 (m, 6H, $-\text{ArOCH}_2\text{Ar}-$), 6.33–6.35 (m, 3H, $-\text{NH}-$), 6.86–7.08 (m, BzI unit aromatic H), 7.33–7.42 (shoulder, tyrosine unit aromatic H).

Branched PEU-8% (*Bis(L-phenylalanine)-Hexane 1,6-Dieste Monomer and Tri-O-benzyl-L-tyrosine-1,1,1-trimethylethane Triester Monomer with a Molar Ratio of 92:8*). ^1H NMR (500 MHz, DMSO- d_6): 0.72–0.76 (m, 3H, $-\text{CCH}_3$), 4.28–4.29 (m, 3H, $-\text{NHCHCOO}-$), 4.99–5.02 (m, 6H, $-\text{ArOCH}_2\text{Ar}-$), 6.33–6.35 (m, 3H, $-\text{NH}-$), 6.86–7.06 (m, BzI unit aromatic H), 7.38–7.42 (shoulder, tyrosine unit aromatic H).

Branched PEU-10% (*Bis(L-phenylalanine)-Hexane 1,6-Dieste Monomer and Tri-O-benzyl-L-tyrosine-1,1,1-trimethylethane Triester Monomer with a Molar Ratio of 90:10*). ^1H NMR (500 MHz, DMSO- d_6): 0.72–0.76 (m, 3H, $-\text{CCH}_3$), 4.26–4.28 (m, 3H, $-\text{NHCHCOO}-$), 4.99–5.02 (m, 6H, $-\text{ArOCH}_2\text{Ar}-$), 6.33–6.34 (m, 3H, $-\text{NH}-$), 6.86–7.08 (m, BzI unit aromatic H), 7.37–7.40 (shoulder, tyrosine unit aromatic H).

Mechanical Property Measurements. Thin films of each polymer were fabricated using a vacuum compression machine (TMP Technical Machine Products Corp.). The machine was

preheated to 160 °C. Then polymer was added into the 5 cm × 5 cm × 0.5 mm mold and put into the compression machine with vacuum on. After 30 min of melting, the system was degassed three times. Next, 10 lbs × 1000, 15 lbs × 1000, 20 lbs × 1000, and 25 lbs × 1000 of pressure were applied for 2 min, respectively. After that, the mold was cooled down with 1000 psi of pressure to prevent the wrinkle on the film's surface. The films were visually inspected to ensure that no bubbles were present in the films. Dumbbell-shaped samples were cut using a custom ASTM Die D-638 Type V.

The elastic modulus of each polymer was obtained using tensile test by Instron (Instron 5543 Universal Testing Machine) at room temperature (25 ± 1 °C). The gauge length was set as 7.25 mm and the crosshead speed was 3 mm/min. The dimensions of the neck of the specimens were 7.11 mm in length, 1.7 mm in width and 0.6 mm in thickness. The elastic moduli were calculated using the slope of linear fitting of the data from strain of 0% to 0.1%. The reported results are average values from three individual measurements.

Water Uptake Measurements. To measure the water uptake characteristics of the polymers, quartz crystal microbalance (QCM, Q-sense E4 operator, Biolin Scientific AB, Sweden) was used. When additional mass is added onto the top of the QCM sensor surface, the resonance frequency of the sensor system will decrease proportional to the mass. The mass change of the materials that attach on the sensor can be calculated from this frequency change based on the Sauerbrey relationship if the materials are rigid.^{58,59}

$$\Delta m = -C \left(\frac{\Delta f}{n} \right)$$

Here Δm is the mass change of the materials on the sensor, C is a constant which is 0.177 mg·Hz⁻¹·m⁻², Δf is the frequency change, and n is the overtone number.

In this experiment, the SiO₂-coated crystal sensors X305 (5 MHz resonant frequency) were cleaned following the standard protocols. A solution (2 wt %) of each polymer in DMF was used to spin coat (2000 rpm for 1 min) thin films on QCM crystals. The spun coat films were annealed at 50 °C in the vacuum for 12 h. Poly(*ε*-caprolactone) was used as a control. To measure the preimmersion thickness of the film, bare QCM sensors and the same QCM sensors following deposition of a polymer film were exposed to the air and resonance frequencies were recorded. On the basis of the Sauerbrey relationship, the preimmersion mass and thickness of the thin film can be calculated based on the frequency shift. The results are the average values for four individual measurements. The preimmersion thickness values were also confirmed with spectroscopic ellipsometry. After known the thickness of the thin films, solvent exchange approach⁵⁹ was carried out to test uptake of water into the polymers as published previously.⁵⁴ The reported results were the average values of four individual measurements. The reported data correspond to the normalized frequency of the seventh overtone.

Nanofiber Fabrication via Electrospinning. Branched PEU-8% was dissolved in hexafluoroisopropanol (HFIP) (6 wt %). A voltage of 12 kV was used and an aluminum foil collector was grounded 15 cm away from the 25 gauge needle. The nanofiber mats were dried in vacuum to remove the residual solvent. The nanofibers were incubated dry at room temperature, dry at 37 °C, dry at 45 °C, soaked in DI water at room temperature for 60 h, soaked in DI water at 37 °C for 60 h, and soaked in DI water at 45 °C for 1 week. The morphology of the nanofibers was characterized using field-emission scanning electron microscopy (SEM) (JSM-7401F, JEOL, Peabody, MA). The acceleration voltage for the SEM imaging was 5.00 kV. Ethylene oxide (EtO) gas treatment was performed using a standard EtO 24 h cycle sterilization apparatus (Andersen Sterilizers, Inc. AN 74i anprolene gas sterilizer). The morphology of the nanofibers after sterilization was also confirmed by SEM. All samples were vacuum-dried at room temperature and sputter coated with silver prior to scanning.

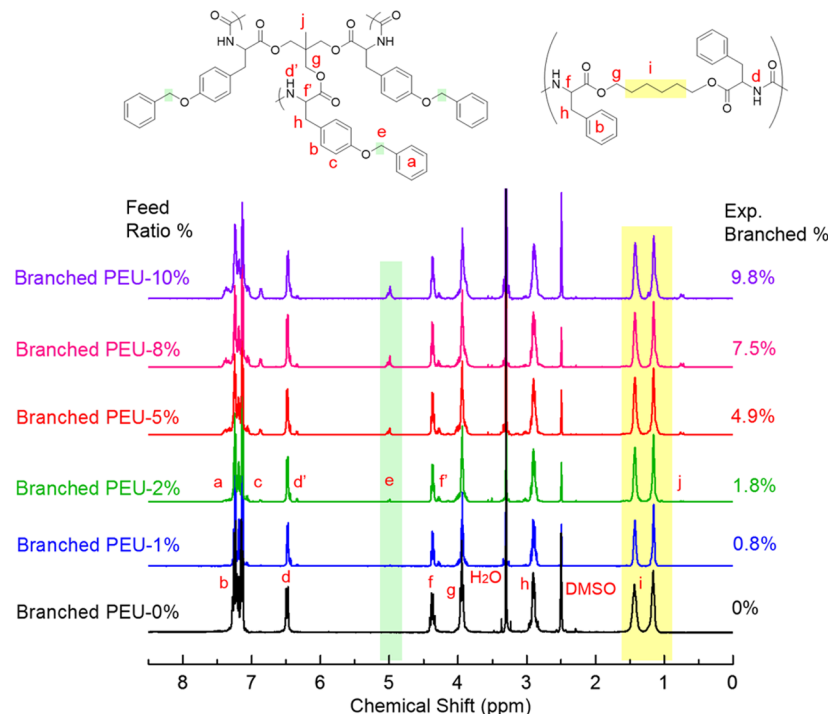


Figure 2. ^1H NMR ($\text{DMSO}-d_6$) of branched poly(ester urea)s (branched PEU-0%, branched PEU-1%, branched PEU-2%, branched PEU-5%, branched PEU-8%, and branched PEU-10%).

RESULTS AND DISCUSSION

Monomer and Polymer Synthesis. Two monomers were synthesized and characterized with ^1H NMR (Figure 1) and ^{13}C NMR (Figure S1). The characteristic resonances of each spectrum demonstrate that each monomer was successfully synthesized. Figure 1a shows the spectrum of linear PEU monomer Diol-PHE, which is the same as the previous published ones.^{51,54,55} For the benzyl-protected tyrosine monomer Triol-TYR in Figure 1b, the aromatic hydrogens of tyrosine have chemical shifts in the range of 6.89–7.42 ppm, which possess different patterns from those of phenylalanine located between 7.09 and 7.50 ppm. The singlet at 5.03 and 0.86 ppm are assigned to the benzyl methylene from benzyl protected tyrosine and methyl group from the triol, respectively. The disappearance of the protons corresponding to the methyl groups in the Boc protecting group at 1.31 ppm and the appearance of resonance associated with the amine group at 8.72 ppm confirms the deprotection process. Both the integration values of individual spectrum (Figure 1) and the ESI results (Figure S2 and Figure S3) show that the monomers are fully functionalized. The FTIR of the monomers (Figure S4) also confirmed the formation of the ester bond. Both monomers are stored as the quantitative amine salt and the free amine is generated *in situ* using sodium carbonate at the beginning of the polymerization.

Random copolymerization using defined feed ratios of linear monomer, Diol-PHE, and branched monomer, Triol-TYR, yielded a series of poly(ester urea)s with different branch densities by interfacial polymerization (Scheme 1). The degree of branching was controlled by the feed ratio of the linear monomer Diol-PHE to the branched monomer Triol-TYR. The chemical structures were characterized by ^1H NMR (Figure 2), ^{13}C NMR (Figure S5) and FTIR spectroscopy (Figure 3). All of the peaks are assigned and the characteristic resonances of each ^1H NMR spectrum show that each of the

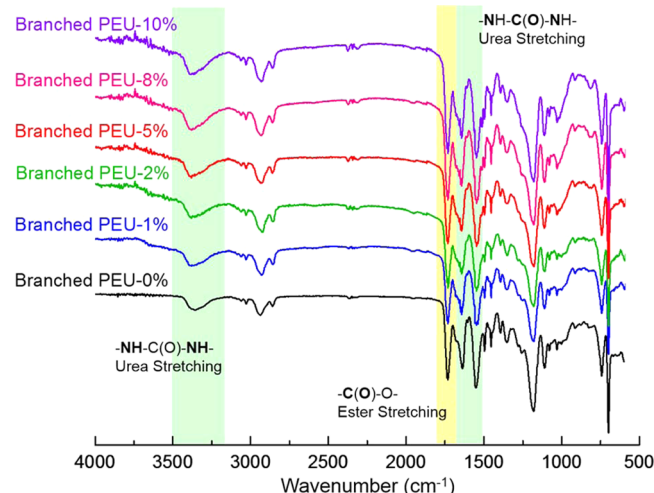


Figure 3. FTIR of branched poly(ester urea)s (branched PEU-0%, branched PEU-1%, branched PEU-2%, branched PEU-5%, branched PEU-8%, and branched PEU-10%).

polymers was successfully synthesized. The spectra of branched PEU-0%, branched PEU-1%, branched PEU-2%, branched PEU-5%, branched PEU-8%, and branched PEU-10% all possess similar chemical shifts except the additional peaks at 0.72–0.76, 4.26–4.29, 4.99–5.02, 6.33–6.35, 6.86–7.08, and 7.33–7.42 ppm which correspond to the signals of the branched monomer Triol-Tyr. The experimentally determined values for the degree of branching can be calculated from the ratio of the following two integration values: the peaks at 4.99–5.02 ppm which correspond to the six benzyl methylene protons from one branched monomer Triol-TYR divided by 6 and the peaks at 1.15–1.43 ppm which represent the eight methylene protons from one linear monomer Diol-PHE divided by 8. The experimental results are listed in Table 1

Table 1. Characterization Data Summary of Branched Poly(ester urea)s with Different Branch Densities

| samples | feed ratio/% | experimental ratio/% | M_w^a | D_M^a | M_w^b | $T_d/^\circ\text{C}$ | $T_g/^\circ\text{C}$ |
|------------------|--------------|----------------------|---------|---------|---------|----------------------|----------------------|
| branched PEU-0% | 0 | 0 | 117k | 1.94 | 68k | 286 | 54 |
| branched PEU-1% | 1 | 0.8 | 65k | 2.19 | 33k | 292 | 57 |
| branched PEU-2% | 2 | 1.8 | 79k | 2.53 | 45k | 301 | 56 |
| branched PEU-5% | 5 | 4.9 | 74k | 2.96 | 38k | 305 | 62 |
| branched PEU-8% | 8 | 7.5 | 108k | 5.31 | 159k | 309 | 62 |
| branched PEU-10% | 10 | 9.8 | 110k | 7.02 | c | 298 | 63 |

^aResults from SEC with RI detector from PS standards. ^bResults from SEC with dual angle light scattering detector (15 and 90°) from a single narrow molecular weight PMMA standard. ^cPolymer does not dissolve well.

and it shows that the values are close to the original feed ratios, which further confirms the successful incorporation of the branched monomers in the polymers. In FTIR spectra (Figure 3), the peaks at 1735–1750 cm⁻¹ correspond to the carbonyl (C=O ester) stretches, which confirms the presence of the ester bond. The C–H (aromatic) stretching at 3000–3100 cm⁻¹, aromatic (C=C aromatic) stretch at 1450–1600 cm⁻¹ and C–H (aromatic) bending at 750 cm⁻¹ show the presence of the aromatic L-phenylalanine and L-tyrosine in the polymer. The strong band at 1000–1300 cm⁻¹ arises from the C–O (ester) stretch and C–H bending vibration. The peaks at 1650–1690 cm⁻¹ are the C=O (urea) stretching peak, which confirms the presence of the urea bond. The peak at 3350–3500 cm⁻¹ is the N–H (urea) stretching peak. All these characteristic signals demonstrate the successful synthesis of the polymers.

The respective molecular masses and postprecipitation molecular mass distributions are listed in Table 1. The polymers are obtained through a step growth polymerization process, which means that the molecular mass distribution should be around 2. However, the reported molecular mass distribution of Branch PEU-0% is 1.94, narrower than the theoretical value for step growth polymerizations. This is because it is a postprecipitation molecular mass and fractionation occurs during precipitation. For the other branched PEUs, they possess higher polydispersity of molecular masses, which is consistent with the properties of branched polymers. The molecular masses of all polymers are sufficiently high for compression molding. All of these polymers are soluble in polar organic solvents, including DMF, dimethyl sulfoxide (DMSO), N-methyl-2-pyrrolidone (NMP), and HFIP. This solubility properties enable a number of solution processing methods such as solution casting, spin coating and electrospinning.

Thermal Properties. TGA results (Table 1) showed that the onset degradation temperatures T_d of the branched poly(ester urea)s are all above 285 °C with subtle differences due to the different amounts of branched monomer incorporated into the copolymer. The PEU polymers possess high thermal stability and their T_d are significantly higher than the glass transition temperature, T_g (Figure 4), which means that these materials can be melt processed with limited thermal degradation processes. The ¹H NMR and SEC results before and after the compression molding were identical, which confirms the materials survive thermal processing (Figure S4 and Table S1).

The DSC (Table 1, Figure 4) results showed that the T_g increases slightly with the low level of branched monomer incorporation. The branched monomer provides less flexibility which lowers the concentrations of the flexible diol in the backbone and possesses large benzyl side groups in the

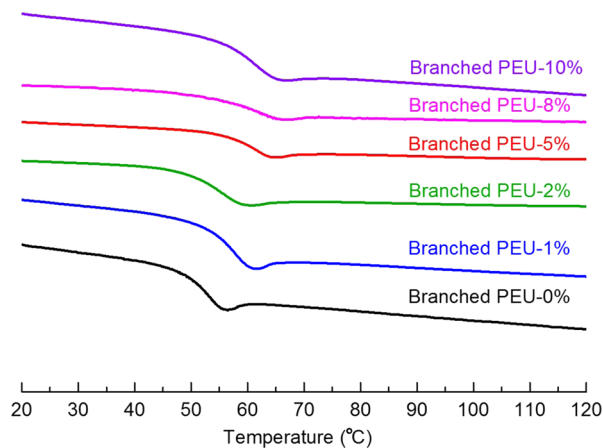


Figure 4. DSC curves of branched poly(ester urea)s (branched PEU-0%, branched PEU-1%, branched PEU-2%, branched PEU-5%, branched PEU-8%, and branched PEU-10%).

branched monomer which can hinder the movement of the backbone chains. These result in the increase in T_g .

Mechanical Properties. The elastic modulus, strain at break and stress at break of branched poly(ester urea)s were characterized by tensile tests at room temperature. The results are reported in Table 2 and Figure 5. The linear fit of the

Table 2. Mechanical Properties of Branched Poly(ester urea)s with Different Branch Densities^a

| | E'/GPa | strain at break/% | stress at break/MPa |
|------------------|-----------------|-------------------|---------------------|
| branched PEU-0% | 3.1 ± 0.1 | 1.7 ± 0.4 | 41.9 ± 4.3 |
| branched PEU-1% | 2.7 ± 0.1 | 2.1 ± 0.3 | 45.0 ± 3.0 |
| branched PEU-2% | 1.9 ± 0.1 | 2.0 ± 0.2 | 38.3 ± 3.5 |
| branched PEU-5% | 1.3 ± 0.1 | 3.4 ± 0.8 | 39.3 ± 8.7 |
| branched PEU-8% | 1.2 ± 0.1 | 4.6 ± 0.9 | 43.9 ± 2.0 |
| branched PEU-10% | 1.0 ± 0.1 | 28.3 ± 1.6 | 24.7 ± 7.3 |

^aThe reported results were the average values of three individual measurements.

respective stress-strain curve values (0% to 0.1%) was used to calculate the elastic modulus. The data showed that the measured values of elastic modulus of branched PEU-0% is identical to values published previously,⁵⁴ and exceeds the published values of clinically available degradable polymers such as PLLA, which is 2.9 GPa.⁵² The branched PEUs possess less mechanical strength compared with linear PEU (branched PEU-0%) due to the decreased strength of the primary structure formed by intersegmental van der Waals forces. With increasing amounts of branched monomer, the decreased regularity of the polymer chains by random copolymerization suppresses the amount of crystallinity. The presence of large

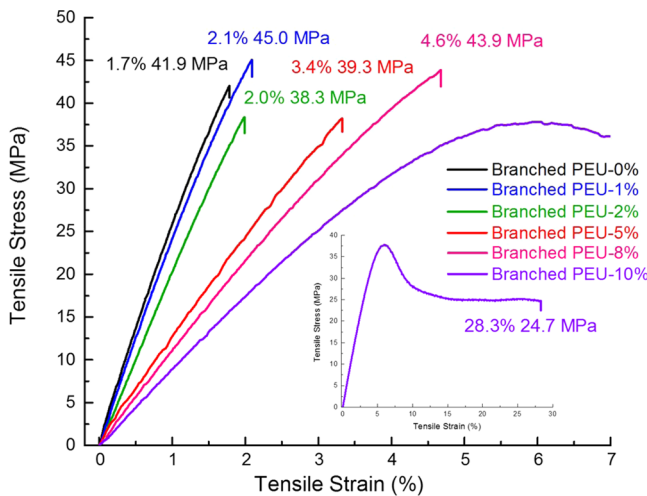


Figure 5. Stress-strain curve for branched poly(ester urea)s measured by Instron 5543 at room temperature ($25 \pm 1^\circ\text{C}$) with dumbbell-shaped samples with the crosshead speed of 3 mm/min. (branched PEU-0%, branched PEU-1%, branched PEU-2%, branched PEU-5%, branched PEU-8%, and branched PEU-10%). The elastic moduli were calculated using the slope of linear fitting of the data from strain 0% to 0.1%. The scale modified plot of branched PEU-10% is shown inside.

benzyl groups in the side chains of the branched monomer reduces intersegmental interactions, which leads to the decreased values of elastic modulus and increased values of elongation at break. The stress-strain curve of branched PEU-10% showed ductile behavior with a yield point at strain of 6.0% and stress of 37.8 MPa. This is likely due to the reduced intersegmental interactions and enhanced chain networks may lead to the brittle to ductile transition.⁶⁰ The elastic modulus of these branched poly(ester urea)s can be tuned by varying the amount of branched monomer. Measurements of mixed compositions of branched monomer with linear polymers and the influence on the resulting chemical and mechanical properties are ongoing.

Water Uptake. The extent of water uptake of polymeric implants is of great importance for applications in biomedicine as water acts as a vehicle for oxygen, nutrition and all the other necessary factors for cells to grow. When polymers are implanted *in vivo*, they are exposed to an aqueous environment. Absorbed water may influence the mechanical and degradation properties as well as dimensional stability. Defects have the potential of compromising function and stability after implantation. Additionally, water uptake provides a measure of the hydrophilic or hydrophobic nature of these materials and the tendency for hydrolytic degradation.⁶¹ The water-uptake

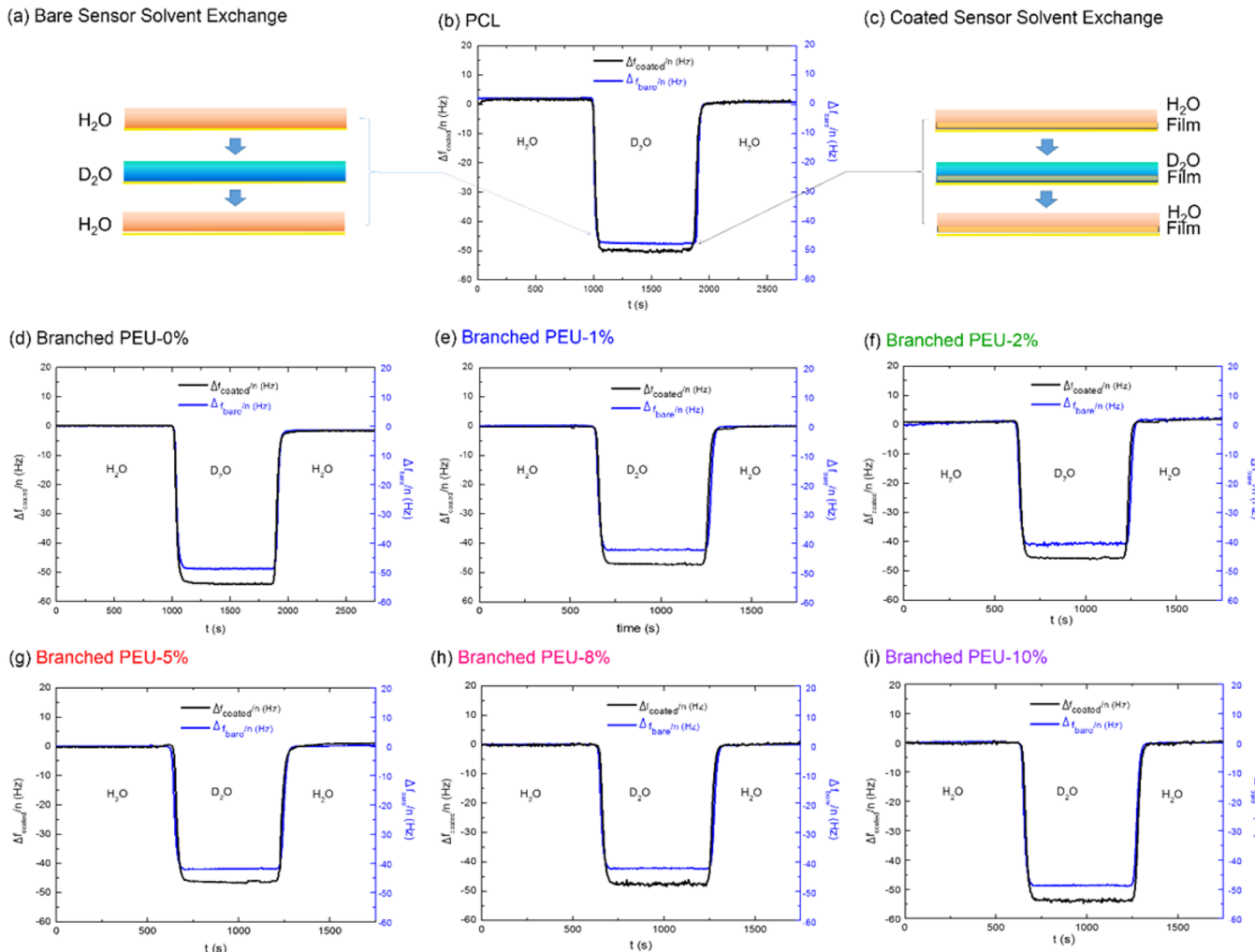


Figure 6. Measurement of water uptake using a solvent exchange approach via QCM. The differences in the scaled frequency changes between the bare crystals and the film-coated crystals are used for the determination of the water content.

traces and level of water uptake of branched PEUs are shown in Figure 6 and Table 3, respectively. To quantify the extent of

Table 3. Extent of Water Uptake of the Branched Poly(ester urea)s with Different Branch Densities

| samples | thickness of the film/nm | water uptake/% |
|------------------|--------------------------|----------------|
| PCL | 52 ± 11 | 0.33 ± 0.09 |
| branched PEU-0% | 41 ± 5 | 1.94 ± 0.07 |
| branched PEU-1% | 38 ± 5 | 2.06 ± 0.02 |
| branched PEU-2% | 37 ± 10 | 2.07 ± 0.04 |
| branched PEU-5% | 46 ± 3 | 2.36 ± 0.07 |
| branched PEU-8% | 39 ± 4 | 2.73 ± 0.12 |
| branched PEU-10% | 39 ± 8 | 3.33 ± 0.06 |

water uptake, polymer films were spun coated onto silicon QCM chips and a solvent exchange procedure for both bare sensors and coated sensors was used. The results showed that the extent of water uptake in branched poly(ester urea)s is limited due to the inherent hydrophobicity. The amount of water uptake increased with increasing degree of branching and the time required to achieve the equilibrium water content decreased. As the amount of branched monomer incorporated into the copolymer increases, the density of the urea groups is higher and the chain packing is less efficient. Comparing with the control group PCL which exhibits the lowest equilibrium water uptake (0.33%), each of the other PEU polymers adsorbs approximately 2% to 3% at the end of a 24 h immersion period.

Nanofibers Processing. Nanofibers of branched PEU-8% were prepared via electrospinning. The fabrication process was stable and continuous. The SEM images confirmed that the morphology of the fibers did not change after soaking in DI water for 60 h and even after ETO sterilization at room temperature (Figure 7, parts a, d, g, and j). If the incubation temperature was changed to 37 °C for the same period of time (60 h), the morphology stayed the same (Figure 7, parts b, e, h, and k), which is very promising for the materials' biomedical applications. If the incubation temperature was increased to 45 °C and the incubation time became longer (1 week), the fibers remained as fibers when they were dry, but appeared to swell and stick to each other when soaked in DI water (Figure 7, parts c, f, i, and l).

CONCLUSION

A series of amino acid-based poly(ester urea) copolymers possessing different degree of branching were synthesized by step growth polymerization. This two-step synthetic route provides a straightforward way to obtain branched poly(ester urea)s in high yield and high molecular mass. The resulting chemical structures were confirmed by ¹H NMR, ¹³C NMR, ESI, and FTIR. TGA and DSC results showed that the branched PEUs possess high thermal stability and higher glass transition temperatures when introducing branched monomers into the copolymer. The tensile test results showed the values of elastic modulus decrease with increasing the degree of branching. The QCM results showed that the linear poly(ester urea)s exhibit a low extent of water uptake and the extent of water uptake increase when increasing the degree of branching. The branched PEUs nanofibers are sterilizable with ETO and are stable for long periods of ETO sterilization, elevated temperature, and exposure to aqueous environment. These enhancements will help to facilitate translation to clinical soft tissue applications.

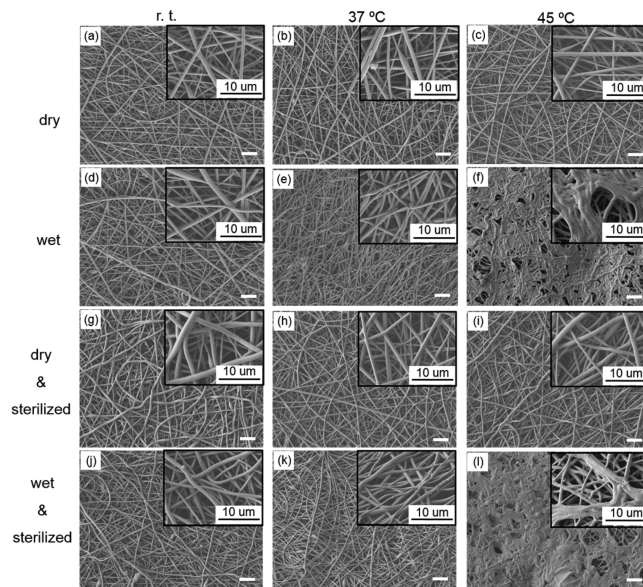


Figure 7. SEM images of branched PEU-8% nanofibers (scale bar 10 μm) dry at room temperature (a), dry at 37 °C (b), dry at 45 °C (c), soaked in DI water at room temperature for 60 h (d), soaked in DI water at 37 °C for 60 h (e), soaked in DI water at 45 °C for 1 week (f), dry at room temperature and ETO sterilized (g), dry at 37 °C and ETO sterilized (h), dry at 45 °C and ETO sterilized (i), soaked in DI water at room temperature for 60 h and ETO sterilized (j), soaked in DI water at 37 °C for 60 h and ETO sterilized (k), and soaked in DI water at 45 °C for 1 week and ETO sterilized (l).

ASSOCIATED CONTENT

S Supporting Information

All synthesis and characterization details of all compounds. This material is available free of charge via the Internet at <http://pubs.acs.org>.

AUTHOR INFORMATION

Corresponding Author

*(M.L.B.) E-mail: becker@uakron.edu.

Notes

The authors declare no competing financial interest.

ACKNOWLEDGMENTS

The authors are grateful to Jianning Liu and Professor Shi-Qing Wang for useful comments, to Dr. Craig Bell and Professor Andrew Dove from the University of Warwick for additional SEC tests, and for financial support from the Akron Functional Materials Center.

REFERENCES

- (1) Frechet, J. M. *Science* **1994**, 263, 1710.
- (2) Inoue, K. *Prog. Polym. Sci.* **2000**, 25, 453.
- (3) Tomalia, D. A.; Fréchet, J. M. J. *J. Polym. Sci., Part A: Polym. Chem.* **2002**, 40, 2719.
- (4) Gao, C.; Yan, D. *Prog. Polym. Sci.* **2004**, 29, 183.
- (5) van Benthem, R. A. T. M. *Prog. Org. Coat.* **2000**, 40, 203.
- (6) Imbesi, P. M.; Gohad, N. V.; Eller, M. J.; Orihuela, B.; Rittschof, D.; Schweikert, E. A.; Mount, A. S.; Wooley, K. L. *ACS Nano* **2012**, 6, 1503.
- (7) Gudipati, C. S.; Greenlieff, C. M.; Johnson, J. A.; Prayongpan, P.; Wooley, K. L. *J. Polym. Sci., Part A: Polym. Chem.* **2004**, 42, 6193.
- (8) Gan, D.; Mueller, A.; Wooley, K. L. *J. Polym. Sci., Part A: Polym. Chem.* **2003**, 41, 3531.

- (9) Matthews, O. A.; Shipway, A. N.; Stoddart, J. F. *Prog. Polym. Sci.* **1998**, *23*, 1.
- (10) Zhou, Y.; Huang, W.; Liu, J.; Zhu, X.; Yan, D. *Adv. Mater.* **2010**, *22*, 4567.
- (11) Khandare, J.; Calderon, M.; Daga, N. M.; Haag, R. *Chem. Soc. Rev.* **2012**, *41*, 2824.
- (12) Kim, T.-i.; Seo, H. J.; Choi, J. S.; Jang, H.-S.; Baek, J.-u.; Kim, K.; Park, J.-S. *Biomacromolecules* **2004**, *5*, 2487.
- (13) Lee, J. H.; Lim, Y.-b.; Choi, J. S.; Lee, Y.; Kim, T.-i.; Kim, H. J.; Yoon, J. K.; Kim, K.; Park, J.-s. *Bioconjugate Chem.* **2003**, *14*, 1214.
- (14) Padilla De Jesús, O. L.; Ihre, H. R.; Gagne, L.; Fréchet, J. M. J.; Szoka, F. C. *Bioconjugate Chem.* **2002**, *13*, 453.
- (15) Zhu, Q.; Qiu, F.; Zhu, B.; Zhu, X. *RSC Adv.* **2013**, *3*, 2071.
- (16) Du, W.; Nyström, A. M.; Zhang, L.; Powell, K. T.; Li, Y.; Cheng, C.; Wickline, S. A.; Wooley, K. L. *Biomacromolecules* **2008**, *9*, 2826.
- (17) Voit, B. I.; Lederer, A. *Chem. Rev.* **2009**, *109*, 5924.
- (18) Kim, Y. H. *J. Polym. Sci., Part A: Polym. Chem.* **1998**, *36*, 1685.
- (19) Mourey, T. H.; Turner, S. R.; Rubinstein, M.; Fréchet, J. M. J.; Hawker, C. J.; Wooley, K. L. *Macromolecules* **1992**, *25*, 2401.
- (20) Kasko, A. M.; Pugh, C. *Macromolecules* **2006**, *39*, 6800.
- (21) Zhou, Y.; Yan, D. *Chem. Commun.* **2009**, 1172.
- (22) Du, W.; Li, Y.; Nyström, A. M.; Cheng, C.; Wooley, K. L. *J. Polym. Sci., Part A: Polym. Chem.* **2010**, *48*, 3487.
- (23) Mitra, A.; Imae, T. *Biomacromolecules* **2003**, *5*, 69.
- (24) Carlmak, A.; Hawker, C.; Hult, A.; Malkoch, M. *Chem. Soc. Rev.* **2009**, *38*, 352.
- (25) Voit, B. *J. Polym. Sci., Part A: Polym. Chem.* **2000**, *38*, 2505.
- (26) Flory, P. J. *J. Am. Chem. Soc.* **1952**, *74*, 2718.
- (27) Kim, Y. H. *J. Am. Chem. Soc.* **1992**, *114*, 4947.
- (28) Hawker, C. J.; Chu, F.; Pomery, P. J.; Hill, D. J. T. *Macromolecules* **1996**, *29*, 3831.
- (29) Kricheldorf, H. R.; Stöber, O. *Macromol. Rapid Commun.* **1994**, *15*, 87.
- (30) Frechet, J. M.; Henmi, M.; Gitsov, I.; Aoshima, S.; Leduc, M. R.; Grubbs, R. B. *Science* **1995**, *269*, 1080.
- (31) Pugh, C.; Singh, A.; Samuel, R.; Bernal Ramos, K. M. *Macromolecules* **2010**, *43*, 5222.
- (32) Wooley, K. L.; Hawker, C. J.; Frechet, J. M. *J. Am. Chem. Soc.* **1991**, *113*, 4252.
- (33) Bharathi, P.; Moore, J. S. *J. Am. Chem. Soc.* **1997**, *119*, 3391.
- (34) Bednarek, M.; Biedron, T.; Helinski, J.; Kaluzynski, K.; Kubisa, P.; Penczek, S. *Macromol. Rapid Commun.* **1999**, *20*, 369.
- (35) Magnusson, H.; Malmström, E.; Hult, A. *Macromol. Rapid Commun.* **1999**, *20*, 453.
- (36) Sunder, A.; Hanselmann, R.; Frey, H.; Mühlaupt, R. *Macromolecules* **1999**, *32*, 4240.
- (37) Kricheldorf, H. R.; Stukenbrock, T. *Polymer* **1997**, *38*, 3373.
- (38) Kricheldorf, H. R.; Stukenbrock, T. *J. Polym. Sci., Part A: Polym. Chem.* **1998**, *36*, 2347.
- (39) Reina, A.; Gerken, A.; Zemann, U.; Kricheldorf, H. R. *Macromol. Chem. Phys.* **1999**, *200*, 1784.
- (40) Li, X.; Zhan, J.; Li, Y. *Macromolecules* **2004**, *37*, 7584.
- (41) van Benthem, R. A. T. M.; Meijerink, N.; Geladé, E.; de Koster, C. G.; Muscat, D.; Froehling, P. E.; Hendriks, P. H. M.; Vermeulen, C. J. A. A.; Zwartkruis, T. J. G. *Macromolecules* **2001**, *34*, 3559.
- (42) Liu, J.; Huang, W.; Zhou, Y.; Yan, D. *Macromolecules* **2009**, *42*, 4394.
- (43) Liu, J.; Huang, W.; Pang, Y.; Zhu, X.; Zhou, Y.; Yan, D. *Biomaterials* **2010**, *31*, 5643.
- (44) Liu, J.; Pang, Y.; Huang, W.; Zhu, X.; Zhou, Y.; Yan, D. *Biomaterials* **2010**, *31*, 1334.
- (45) Huang, S. J.; Bansleben, D. A.; Knox, J. R. *J. Appl. Polym. Sci.* **1979**, *23*, 429.
- (46) Zimmermann, J.; Loontjens, T.; Scholtens, B. J. R.; Mühlaupt, R. *Biomaterials* **2004**, *25*, 2713.
- (47) Marcos-Fernández, A.; Abraham, G. A.; Valentín, J. L.; Román, J. S. *Polymer* **2006**, *47*, 785.
- (48) Kartvelishvili, T.; Tsitlanadze, G.; Edilashvili, L.; Japaridze, N.; Katsarava, R. *Macromol. Chem. Phys.* **1997**, *198*, 1921.
- (49) Strable, E.; Prasuhn, D. E.; Udit, A. K.; Brown, S.; Link, A. J.; Ngo, J. T.; Lander, G.; Quispe, J.; Potter, C. S.; Carragher, B.; Tirrell, D. A.; Finn, M. G. *Bioconjugate Chem.* **2008**, *19*, 866.
- (50) Kasuga, T.; Ota, Y.; Nogami, M.; Abe, Y. *Biomaterials* **2000**, *22*, 19.
- (51) Stakleff, K. S.; Lin, F.; Smith Callahan, L. A.; Wade, M. B.; Esterle, A.; Miller, J.; Graham, M.; Becker, M. L. *Acta Biomaterialia* **2013**, *9*, 5132.
- (52) Duek, E. A. R.; Zavaglia, C. A. C.; Belanger, W. D. *Polymer* **1999**, *40*, 6465.
- (53) Policastro, G. M.; Lin, F.; Smith Callahan, L. A.; Esterle, A.; Graham, M.; Stakleff, K. S.; Becker, M. L. *Biomacromolecules* **2015**, *16*, 1358.
- (54) Yu, J.; Lin, F.; Lin, P.; Gao, Y.; Becker, M. L. *Macromolecules* **2014**, *47*, 121.
- (55) Lin, F.; Yu, J.; Tang, W.; Zheng, J.; Xie, S.; Becker, M. L. *Macromolecules* **2013**, *46*, 9515.
- (56) Li, S.; Yu, J.; Wade, M. B.; Policastro, G. M.; Becker, M. L. *Biomacromolecules* **2015**, *16*, 615.
- (57) Pang, X.; Chu, C.-C. *Biomaterials* **2010**, *31*, 3745.
- (58) Sauvrebry, G. Z. *Phys.* **1959**, 206.
- (59) Aulin, C.; Ahola, S.; Josefsson, P.; Nishino, T.; Hirose, Y.; Österberg, M.; Wågberg, L. *Langmuir* **2009**, *25*, 7675.
- (60) Zartman, G. D.; Cheng, S.; Li, X.; Lin, F.; Becker, M. L.; Wang, S.-Q. *Macromolecules* **2012**, *45*, 6719.
- (61) Hooper, K. A.; Macon, N. D.; Kohn, J. *J. Biomed. Mater. Res.* **1998**, *41*, 443.